Acta Crystallographica Section D
Biological Crystallography
ISSN 0907-4449

Structure of the zinc-induced heterodimer of two calcium-free isoforms of phospholipase A_2 from *Naja naja sagittifera* at 2.7 Å resolution

Talat Jabeen, Sujata Sharma, Nagendra Singh, Rajendra K. Singh, Ashok K. Verma, M. Paramasivam, A. Srinivasan and Tej P. Singh*

Department of Biophysics, All India Institute of Medical Sciences, New Delhi 110029, India

Correspondence e-mail: tps@aiims.aiims.ac.in

Received 13 November 2004
Accepted 14 December 2004

PDB Reference: phospholipase A_2, 1xxw, r1xxwsf.

The crystal structure of a zinc-induced heterodimer of two metal-free isoforms of a cobra venom phospholipase A_2 has been determined at 2.7 Å resolution. The crystals belong to space group $P4_1$, with unit-cell parameters $a = b = 65.5$, $c = 58.4$ Å, and have a single dimer in the asymmetric unit. The structure has been refined to R_{cryst} and R_{free} factors of 0.188 and 0.232, respectively. The two isoforms have a sequence identity of 82%. The zinc ion forms a fivefold coordination with a trigonal bipyramidal geometry involving one O atom each from Asp24 and Asn112 from molecule *A* and Asp24 from molecule *B* and two water molecules. Both molecules of the dimer are inactive. Molecule *A* is inactive because Arg31 (*B*) binds to Asp49 (*A*), while an acetate ion has displaced the essential water molecule and interacts with His48 (*A*). On the other hand, Arg31 (*A*) interacts with the calcium-binding loop of molecule *B*, resulting in an altered conformation of the loop. The absence of a calcium ion, loss of the essential water molecule and the altered conformation of the calcium-binding loop may be the reasons for the loss of activity of molecule *B*.

1. Introduction

Phospholipase A_2 (PLA_2, phosphatide acylhydrolase; EC 3.1.1.4) enzymes hydrolyze phospholipids at the *sn*-2 position (van Deenen & de Haas, 1963; Dennis, 1997). The pharmacological interest in this reaction arises from the fact that PLA_2 may catalyze the release of arachidonic acid and hence may participate in the inflammatory cascade involving prostaglandins, thromboxanes and leukotrienes (Saiga *et al.*, 2001; Leistad *et al.*, 2004). Excess production of these compounds is assumed to be responsible for various chronic inflammatory diseases such as rheumatoid arthritis and asthma (Zurier, 1975; Kojima *et al.*, 2003). Inhibitors of various enzymes of the cascade including PLA_2 are thus expected to reduce the effects of inflammation. It has been shown that the inhibitors of both human and snake-venom PLA_2s display a similar mode of binding through similar substrate-recognition hydrophobic channels (Bryant *et al.*, 1999; Singh *et al.*, 2003). Therefore, using venom PLA_2s for the purpose of understanding the mechanism of binding of various ligands including metal ions is generally acceptable. So far, the binding of a number of natural compounds (Chandra, Jasti, Kaur, Betzel *et al.*, 2002; Chandra, Jasti, Kaur, Srinivian *et al.*, 2002), non-steroidal anti-inflammatory drugs (Singh *et al.*, 2004) and designed peptides (Chandra, Jasti, Kaur, Dey, Perbandt *et al.*, 2002; Chandra, Jasti, Kaur, Dey, Srinivasan *et al.*, 2002; Singh *et al.*, 2003) have been analyzed. However, the effects of metal ions other than calcium have not been studied thus far.

It has generally been observed that the catalytic activity of PLA_2 requires the presence of a calcium ion in the calcium-binding loop (Jesse & Franson, 1979; Chang *et al.*, 1996). The calcium ion supports the structure of the calcium-binding loop, which forms one of the walls of the substrate-binding hydrophobic channel. It also contributes to creating a desirable electronic environment through Asp49 for the residues of the active site, *i.e.* His48, Tyr52 and Asp94. Some recent structural reports have indicated that in some isoforms of PLA_2 calcium ion may not be absolutely essential for their function (Perbandt *et al.*, 1997; Chandra *et al.*, 2001; Banumathi *et al.*, 2001). There is yet another aspect of the role of the metal ion in that it may also contribute to the inactivity of PLA_2 enzymes by inducing specific oligomerization of certain PLA_2 isoforms. However, the lack of structural studies on the involvement of metal ions within PLA_2 molecules is a serious lacuna. In order to understand the structural role of metal ions such as Zn^{2+}, Mg^{2+} *etc*., we report here the crystal structure of the zinc-induced heterodimer of two isoforms of phospholipase A_2 from *Naja naja sagittifera*. The crystal structure shows that the Zn^{2+} ion fails to bind in the calcium-binding loop of either of the two PLA_2 molecules. However, Zn^{2+} is found at the interface of the heterodimer with a pentagonal bipyramidal coordination geometry involving Asp24 and Asn112 from molecule *A*, Asp24 from molecule *B* and two water molecules. The observed conformations of the calcium-binding loops and the orientations of the Arg31 side chains of the two molecules differ considerably. Kinetic studies show that the heterodimer does not possess PLA_2 activity.

Table 1
Data-collection and refinement statistics.

Values in parentheses are for the high-resolution shell (2.75–2.70 Å).

PDB code	1xxw
Space group	$P4_1$
Unit-cell parameters (Å)	
$a = b$	65.5
c	58.4
V_M (Å^3 Da^{-1})	2.2
Solvent content (%)	45
Z	8
Resolution range (Å)	20.0–2.7
Total No. of measured reflections	56251
No. of unique reflections	6887
Completeness (%)	99.0 (98.0)
Overall R_{sym} (%)	11.0 (20.0)
Overall $I/\sigma(I)$	9.9 (2.7)
R_{cryst} (%)	18.8
R_{free} (%)	23.2
Protein atoms	1837
Zinc ion	1
Acetate ions	2
Water molecules	194
R.m.s.d. in bond lengths (Å)	0.008
R.m.s.d. in bond angles (°)	1.3
R.m.s.d. in torsion angles (°)	22.2
Overall G factor	0.19
B factor estimated from Wilson plot (Å^2)	36.0
Mean B factor for main-chain atoms (Å^2)	35.8
Mean B factor for side-chain atoms and water O atoms (Å^2)	38.4
Mean B factor for all atoms (Å^2)	37.2
Residues in most allowed regions (%)	87.0
Residues in additionally allowed regions (%)	11.1
Residues in generously allowed regions (%)	1.9

2. Material and methods

2.1. Isolation and purification

Lyophilized samples of cobra venom were obtained from the Irula Snake Catchers Industrial Cooperative Society, Chennai, India. The venom was dissolved in 50 m*M* Tris–HCl, 100 m*M* NaCl pH 7.0 at 50 mg ml^{-1} concentration by stirring it for 30 min at 298 K. The solution was cleared by centrifugation at 12 000*g* for 10 min and size-fractionated on a Sephadex G-150 column pre-equilibrated with 50 m*M* Tris–HCl, 100 m*M* NaCl pH 7.0. The column was eluted with the same buffer at a flow rate of 6 ml h^{-1}. The elution profile showed five peaks. The peak corresponding to a molecular weight of 14 kDa on sodium dodecyl sulfate–polyacrylamide gel electrophoresis (SDS–PAGE) was pooled for further purification.

The pooled fractions were desalted and dialyzed against 50 m*M* Tris–HCl pH 7.0 and loaded onto a carboxymethyl C-50 column. The column was washed with the above buffer. The unbound fractions were pooled and dialyzed against 50 m*M* ammonium acetate buffer pH 6.0. This was finally loaded onto a Cibacron blue affinity column pre-equilibrated with 50 m*M* ammonium acetate pH 6.0 and dialyzed against the same buffer. The column was washed with the same buffer. The column was first eluted with 50 m*M* ammonium bicarbonate pH 8.0 and then with 20 m*M* ammonium carbonate pH 10.5. The fractions eluted by 50 m*M* ammonium bicarbonate pH 8.0 showed PLA_2 activity and indicated a molecular weight of 14 kDa on SDS–PAGE. These fractions were pooled, ultrafiltered and lyophilized. The sequences of both monomers were determined using cDNA and deposited in the GenBank with accession Nos. AY422775 and AY422776.

2.2. Dynamic light scattering

Dynamic light-scattering (DLS) measurements were made at various concentrations of protein containing two isoforms in the presence and absence of zinc ions. This experiment was also repeated in the presence and absence of calcium and magnesium ions. The studies were carried out with a DLS system (RiNA, Berlin, Germany) and analyzed using the software described by Schulze (1996). The sample solutions were prepared in 10 m*M* sodium phosphate buffer pH 6.0 made using deionized water from a Millipore Alpha-Q system. The samples were filtered through 0.1 µm polyvinylidene difluoride filters (Millipore). The protein concentration used was 10 mg ml^{-1} at a constant temperature. The samples were manually injected into the flow cell (50 µl) and illuminated with a 25 mW, 600 nm solid-state laser. The data for the hydrodynamic radii were measured three times and averaged.

2.3. Kinetic studies

The purified enzyme was used for kinetic studies. In the kinetic experiments, the 1,2-dithio analogue of diheptanoyl

phosphatidylcholine was used as a substrate (PLA_2 assay kit, Cayman Chemicals, Michigan, USA). Upon hydrolysis of the thioester bond at the *sn*-2 position by PLA_2, free thiols are liberated which are detected using 5,5′-dithiobis-(2-nitrobenzoic acid) (DTNB). The assay was performed in 20 m*M* sodium cacodylate buffer pH 7.0 at 298 K. The enzyme concentrations were fixed at 10 mg ml^{-1}, while the concentrations of $ZnCl_2$ were varied from 0 to 20 m*M*. A 1 m*M* concentration of substrate was added to initiate the reaction. The resulting products were estimated by the differences in absorbance at 414 nm.

2.4. Crystallization

The purified and lyophilized protein samples were used for crystallization experiments. The hanging-drop vapour-diffusion method was used for the initial screening of crystallization conditions. Since the PLA_2 was treated with zinc acetate and behaved somewhat differently, several crystallization conditions were initially tried. The best crystals were finally obtained by dissolving the protein at a concentration of 10 mg ml^{-1} in 10 m*M* sodium cacodylate buffer pH 6.5 and equilibrating against the same buffer containing 25% ethanol.

2.5. Data collection

The crystals were stable in the X-ray beam for up to 24 h. One crystal with dimensions 0.4 × 0.2 × 0.2 mm was used for X-ray intensity data collection at 278 K with a 300 mm diameter MAR Research imaging-plate scanner mounted on an RU-200 rotating-anode X-ray generator equipped with a graphite monochromator. The intensities were integrated using *DENZO* and *SCALEPACK* (Otwinowski & Minor, 1997). The crystals belong to space group $P4_1$ ($P4_3$ was ruled out at the stage of structure determination and refinement), with unit-cell parameters $a = b = 65.5$, $c = 58.4$ Å and four molecules in the unit cell. The data have an overall R_{sym} of 11.0% with an overall completeness of 99% to 2.7 Å resolution. The statistics of the crystallographic data are listed in Table 1.

2.6. Structure determination and refinement

The structure was determined by molecular replacement method with *Auto-AMoRe* (Navaza, 1994) using the coordinates of a group I PLA_2 from *N. naja naja* (PDB code 1psh) as the search model. The rotation and translation functions calculated with data in the resolution range 12.0–4.0 Å yielded a clear solution with the first two peaks being distinct. The stacking arrangement of the molecules in the unit cell for this

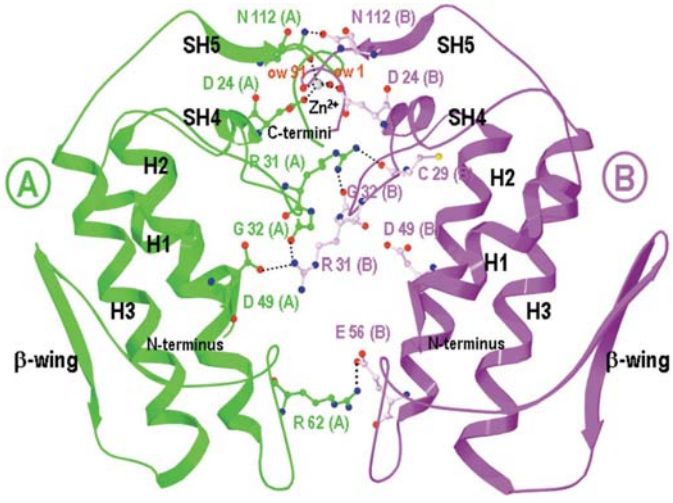

Figure 2
The overall structure of the heterodimer, indicating the site of zinc coordination. The important residues involved in intermolecular interactions are also shown.

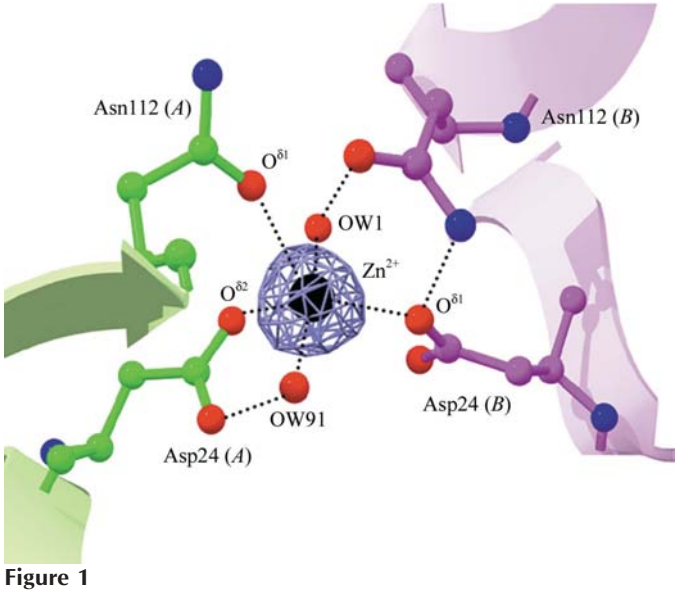

Figure 1
Difference $|F_o - F_c|$ electron density for the zinc ion drawn at 4σ. The zinc ion is located at the interface of molecules *A* and *B*. All figures were drawn using the program *Swiss PDB Viewer* (Guex & Peitsch, 1997).

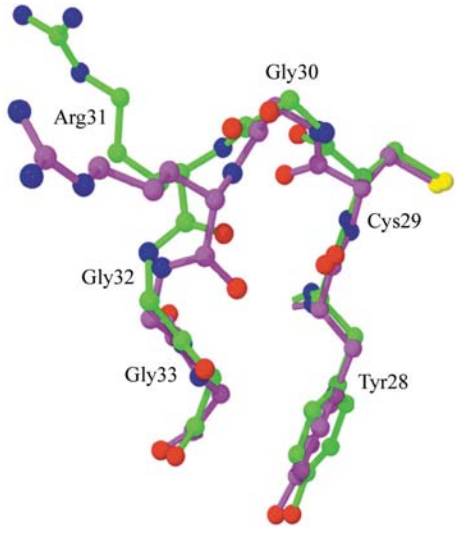

Figure 3
Superimposition of the calcium-binding loop of molecule *A* (green) on that of molecule *B* (magenta).

solution yielded no unfavourable intermolecular contacts. The coordinates transformed using *AMoRe* (Navaza, 1994) were subjected to 20 cycles of rigid-body refinement with *REFMAC*5 (Murshudov & Dodson, 1997) from the *CCP*4*i* v.4.2 software suite (Collaborative Computational Project, Number 4, 1994). This reduced the R_{cryst} factor to 34.3% with an R_{free} of 42.1% (5% of the reflections were used for the calculation of R_{free} and were not included in the refinement). The manual model building of the protein into ($|2F_o - F_c|$) and ($|F_o - F_c|$) electron-density maps was carried out with the graphics program *O* (Jones *et al.*, 1991) on a Silicon Graphics O2 workstation. One zinc ion was identified at the intermolecular site between residues Asp24 from the two molecules (Fig. 1). Water molecules were added using *ARPP*/*REFMAC* (Collaborative Computational Project, Number 4, 1994). Two acetate ions were located, one at the surface of molecule *A* and the other in its active site. Further refinement with additional water molecules was carried out until all peaks in the difference Fourier ($|F_o - F_c|$) map were fully explained. The water molecules were adjusted manually for good hydrogen-bonding geometry with protein atoms using the program *O* (Jones *et al.*, 1991). The final set of refined coordinates consists of 1837 protein atoms from the two PLA_2 molecules, one zinc and two acetate ions and 191 water molecules with good geometry. The final R_{cryst} and R_{free} factors were 0.188 and 0.232, respectively, for data in the resolution range 20.0–2.7 Å.

3. Results and discussion

3.1. Molecular association

The results of the dynamic light-scattering (DLS) experiments indicated a mean hydrodynamic radius (R_H) of 1.9 ± 0.1 nm without any zinc ions. In the presence of zinc, the R_H value was found to be 2.6 ± 0.1 nm. The R_H values of 1.9 and 2.6 nm correspond to proteins of molecular weights 14 and 28 kDa, respectively (Dahneke, 1983; Schmitz, 1990). Since

Table 2
A comparison of distances to calcium and zinc cations in the PLA_2 heterodimers.

Calcium coordination	Distances (Å)	Zinc coordination	Distances (Å)
Asp24 (*A*) $O^{\delta1}$	2.64	—	—
Asp24 (*A*) $O^{\delta2}$	2.60	Asp24 (*A*) $O^{\delta2}$	2.24
Asn112 (*A*) $O^{\delta1}$	2.29	Asn112 (*A*) $O^{\delta1}$	2.41
Asp24 (*B*) $O^{\delta1}$	2.30	Asp24 (*B*) $O^{\delta1}$	2.15
Asn112 (*B*) $O^{\delta1}$	2.38	—	—
OW144	2.29	OW1	2.17
OW148	2.28	OW91	2.15

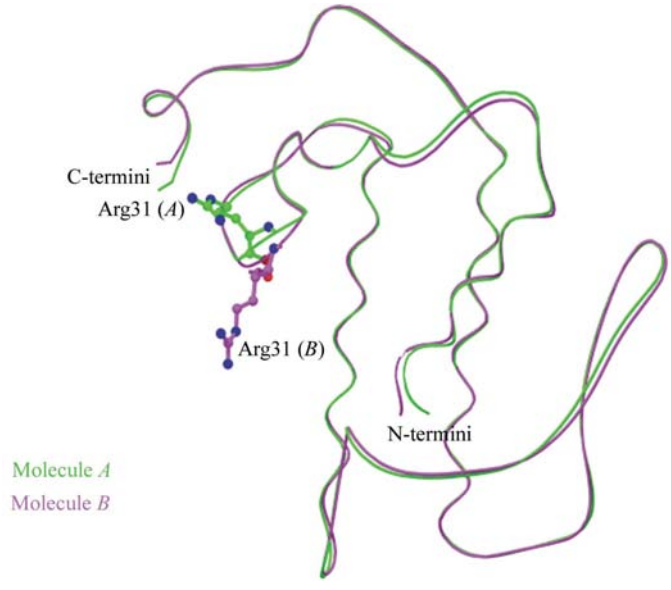

Figure 4
The superimposition of C^{α} traces of molecule *A* on that of molecule *B*. The side chains of Arg31 (*A*) and Arg31 (*B*) are shown to indicate the differences in the orientations.

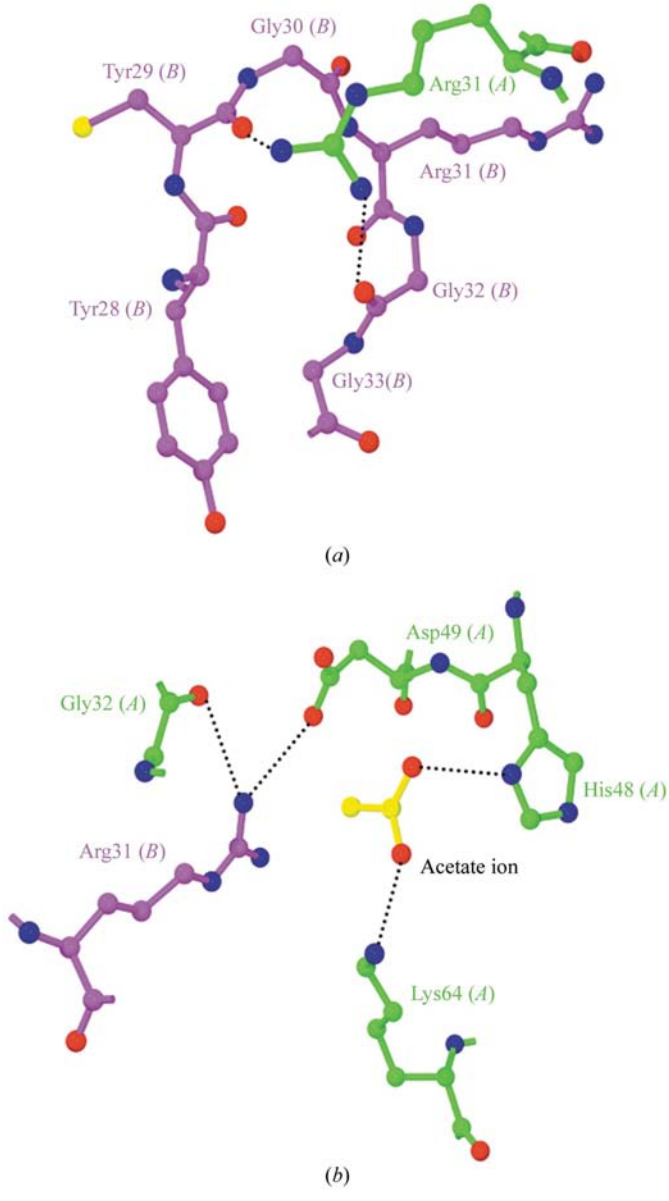

Figure 5
(*a*) Calcium-binding loop of molecule *B* together with Arg31 (*A*) and interactions between them. (*b*) The interactions between Arg31 (*B*) and Asp49 (*A*) and between acetate ion and His48 (*A*) and Lys64 (*A*).

Table 3
Hydrogen-bonding interactions between the monomers.

Molecule *A*	Molecule *B*	Distance (Å)
Arg31 NH2	Cys29 O	2.74
Arg31 NH2	Gly32 O	2.86
Gly32 O	Arg31 NH1	3.21
Asp49 $O^{\delta2}$	Arg31 NH1	3.18
Arg62 NH1	Glu56 $O^{\delta1}$	3.40
Asn112 $N^{\delta2}$	Asn112 $O^{\delta1}$	3.23
Asp114 $O^{\delta1}$	Tyr111 OH	3.08
Lys116 N^{ζ}	Asp21 $O^{\delta1}$	2.70
Lys116 N^{ζ}	Asp21 $O^{\delta2}$	3.16

the polydiversity value in these estimates was below 15% of the average radius, all PLA_2 molecules in the two experiments existed in single forms. Thus, it was clearly understood that these samples of PLA_2 existed in a dimeric form in the presence of zinc ion. Similar results were obtained in the presence of calcium and magnesium ions.

3.2. Effect of zinc ions on the activity of PLA_2

It is well known that a calcium ion plays an important role in the activity/inactivity cycle of PLA_2 enzymes. Surprisingly, the effects of other metal ions on PLA_2 activity have not been studied structurally, although the effects of some divalent cations on the activity of PLA_2 have been reported (Aleksiev & Tchorbanov, 1976). The mixture of two isoforms in the absence of calcium ions showed no activity. Normal PLA_2 activity was indicated in the presence of calcium ions (Jabeen *et al.*, 2005), but in the case of zinc ions the enzyme showed no PLA_2 activity at all metal-ion concentrations. It is noteworthy that the enzyme samples were found in the monomeric form without zinc ions and were transformed into the dimeric form in the presence of zinc ions. This indicated that a zinc ion did not bind to PLA_2 at the calcium-binding loop and was able to induce dimerization in a similar manner to that observed with calcium ions (Jabeen *et al.*, 2005).

3.3. Quality of the model

The final model represents a well defined protein chain based on the high-quality ($|2F_o - F_c|$) electron-density maps. The overall *G* factor calculated by *PROCHECK* (Laskowski *et al.*, 1993) as a measure of stereochemical quality of the model was 0.15. 86.5% of the non-glycine and non-proline residues fall into the most favoured regions of the Ramachandran plot (Ramachandran & Sasisekaran, 1968). The statistics of the structure refinement are given in Table 1.

3.4. Structure of the dimer

The structure contains a zinc-induced dimer. The two isoforms show an identity of 82% in their amino-acid sequences. The majority of differences are conservative and occur between Cys61 and Val90 encompassing the β-wing. The residue that occurs commonly at position 2 is Leu/Ile and is involved in promoting the hydrophobic environment of the substrate-binding site. This is important for the diffusion of substrate into the substrate-binding site of PLA_2. In the heterodimer, the two monomers contain Thr2 and Arg2, respectively. These differences are expected to have important functional implications. The two molecules of the dimer will subsequently be referred to as molecules *A* and *B*. The overall structure of the heterodimer is illustrated in Fig. 2. The molecular topology of both PLA_2 molecules conserves all main features of the PLA_2 type of folding. The N-terminal helix H1 runs from residue 2 to residue 12. Helix 2 (H2) extends from residue 40 to residue 55 and helix 3 (H3) spans residues 85–103. The structure also contains a double-stranded antiparallel β-wing (residues 70–73 and 76–79). There are two helical turns involving residues 19–22 (SH4) and 110–112 (SH5). The zinc ion is involved in coordination with molecules *A* and *B* through Asp24 (*A*) $O^{\delta2}$, Asn112 (*A*) $O^{\delta1}$, Asp24 (*B*) $O^{\delta2}$ and two water molecules OW1 and OW91. These interactions give rise to a pentagonal bipyramidal coordination geometry. In the calcium-induced dimer, the calcium ion is located at the same site and forms a sevenfold coordination (Jabeen *et al.*, 2005) (Table 2). The backbone conformations of molecules *A* and *B* are essentially similar; the r.m.s. displacement of C^{α} traces is 0.6 Å. Similarly, the least-squares superpositions of C^{α} atoms of the zinc dimer on equivalent C^{α} atoms of the calcium dimer (PDB code 1s6b; Jabeen *et al.*, 2005) also shows an r.m.s. shift of 0.6 Å. Molecules *A* and *B* in the zinc dimer associate lengthwise and are held together by interactions at three distinct sites (Table 3). At one end the zinc ion forms a fivefold coordination. In the central part of the interface, Arg31 (*A*) interacts with Cys29 (*B*) and Gly32 (*B*) and Arg31 (*B*) binds to Asp49 (*A*) and Gly32 (*A*), while at the third site a salt bridge is observed between Arg62 (*A*) and Glu56 (*B*).

3.5. Comparison of the calcium-binding loops

The calcium-binding loops of the two monomers show notable differences in the orientations of Arg31, although the calcium-binding loops in both molecules are devoid of metal ions (Fig. 3). The Tyr28 side chains in molecules *A* and *B* are rotated almost by 90° with respect to each other. The overall folding of the calcium-binding loops also differ significantly: the loop in molecule *B* has a considerably smaller width than that in molecule *A*. In fact, the width of the calcium-binding loop of molecule *B* is one of the smallest widths of a calcium-binding loop observed in any PLA_2 structure. Comparable loop sizes have also been observed in two other heterodimers of PLA_2 (Jabeen *et al.*, 2005; Perbandt *et al.*, 1997). These results clearly indicate that the calcium-binding loop is indeed a flexible part of the protein chain and adopts different conformations in the absence of calcium ions. Furthermore, the presence of an Arg residue at position 31 of the calcium-binding loop indicates important functional implications of PLA_2 through dimerization and altered conformation of the loop which forms a wall of the hydrophobic substrate-binding channel.

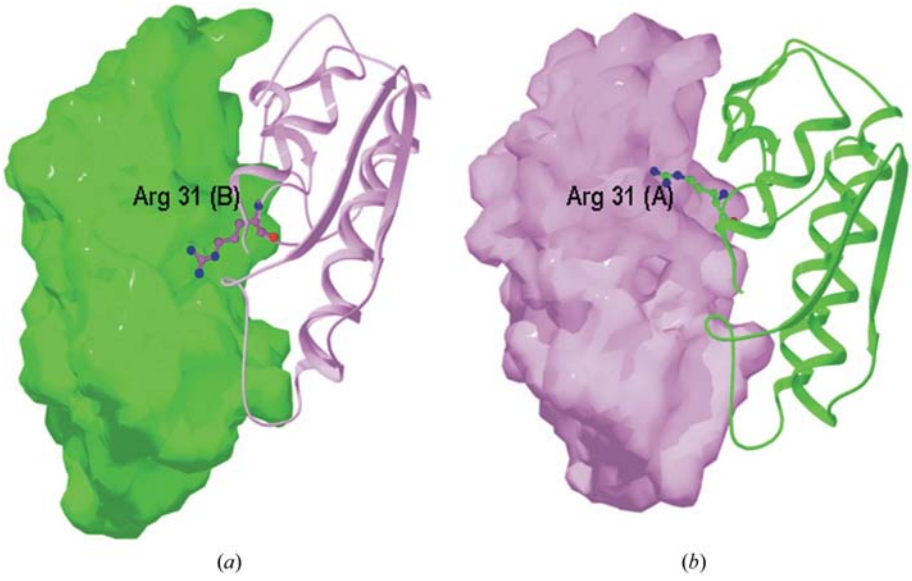

Figure 6
Association of molecules *A* and *B*: (*a*) molecule *A* in *GRASP* surface representation with Arg31 (*B*) intruding into the body of molecule *A* and (*b*) molecule *B* in *GRASP* surface representation with Arg31 (*A*) penetrating into the body of molecule *B*.

3.6. Roles of Arg31

The presence of Arg31 is a unique feature of cobra venom PLA_2s. As seen in Fig. 4, the Arg31 residues of molecules *A* and *B* are oriented differently. The Arg31 (*A*) guanidinium group intrudes into the calcium-binding loop of molecule *B* and forms hydrogen bonds with the carbonyl O atoms of Cys29 (*B*) and Gly32 (*B*) (Fig. 5*a*). This role of the Arg31 residue reduces the scope of binding of the calcium ion by the calcium-binding loop of molecule *A*. On the other hand, Arg31 (*B*) interacts directly with the active-site residues of molecule *A*, forming an electrostatic interaction with Asp49 and a hydrogen bond with Gly32 (*A*) O (Fig. 5*b*). The acetate ion forms a bridge between Lys64 (*A*) and His48 (*A*), thus further helping in the inactivation of molecule *A*. Overall, the observed novel interactions involving Arg31 (*A*) and Arg31 (*B*) seem to be critical for stabilizing the dimer induced by the Zn^{2+} ion and result in the inactivation of both molecules *A* and *B* (Fig. 6).

4. Conclusions

The crystal structure of the zinc-induced heterodimer of two isoforms of cobra venom PLA_2 clearly shows that a zinc ion is capable of inducing dimerization in some isoforms of PLA_2, leading to the inactivation of both isoforms. It has been observed that Zn^{2+} is unable to bind in the calcium-binding loop of PLA_2, indicating that the loop is specific to calcium ions. The presence of an Arg residue at position 31 in PLA_2 molecule is important in the dimerization of these two isoforms of PLA_2 as well as in their inactivation. The dimerization induced by divalent zinc ions may also occur with other divalent cations (Aleksiev & Tchorbanov, 1976). Recently, the crystal structure of a calcium-induced heterodimer of two isoforms has been reported (Jabeen *et al.*, 2005). There seems to be a general trend that the presence of an Arg/Lys residue at position 31 position requires calcium ions for PLA_2 activity, while PLA_2s containing non-basic residues at position 31 can be active without calcium ions.

The authors acknowledge financial assistance from the Department of Science and Technology, New Delhi under the FIST programme. TJ, NS and RKS thank the Council of Scientific and Industrial Research, New Delhi for the award of fellowships.

References

Aleksiev, B. & Tchorbanov, B. (1976). *Toxicon*, **14**, 477–485.
Banumathi, S., Rajashankar, K. R., Notzel, C., Aleksiev, B., Singh, T. P., Genov, N. & Betzel, C. (2001). *Acta Cryst.* D**57**, 1552–1559.
Bryant, M. D., Flick, K. E., Koduri, R. S., Wilton, D. C., Stoddard, B. L. & Gelb, M. H. (1999). *Bioorg. Med. Chem. Lett.* **9**, 1097–1102.
Chandra, V., Jasti, J., Kaur, P., Betzel, C., Srinivasan, A. & Singh, T. P. (2002). *J. Mol. Biol.* **320**, 215–222.
Chandra, V., Jasti, J., Kaur, P., Dey, S., Perbandt, M., Srinivasan, A., Betzel, C. & Singh, T. P. (2002). *J. Biol. Chem.* **277**, 41079–41085.
Chandra, V., Jasti, J., Kaur, P., Dey, S., Srinivasan, A., Betzel, C. & Singh, T. P. (2002). *Acta Cryst.* D**58**, 1813–1819.
Chandra, V., Jasti, J., Kaur, P., Srinivasan, A., Betzel, C. & Singh, T. P. (2002). *Biochemistry*, **41**, 10914–10919.
Chandra, V., Kaur, P., Jasti, J., Betzel, C. & Singh, T. P. (2001). *Acta Cryst.* D**57**, 1793–1788.
Chang, L. S., Lin, S. R. & Chang, C. C. (1996). *J. Protein Chem.* **15**, 701–707.
Collaborative Computational Project, Number 4 (1994). *Acta Cryst.* D**50**, 760–763.
Dahneke, B. E. (1983). *Measurement of Suspended Particles by Quasi-Elastic Light Scattering*, pp. 199–236. New York: Wiley.
Deenen, L. L. M. van & de Haas, G. H. (1963). *Biochem. Biophys. Acta*, **70**, 538–553.
Dennis, E. A. (1997). *Trends Biochem. Sci.* **22**, 1–2.
Guex, N. & Peitsch, M. C. (1997). *Electrophoresis*, **18**, 2714–2723.
Jabeen, T., Sharma, S., Singh, N., Singh, R. K., Kaur, P., Perbandt, M., Betzel, C., Srinivasan, A. & Singh, T. P. (2005). In the press.
Jesse, R. L. & Franson, R. C. (1979). *Biochim. Biophys. Acta*, **575**, 467–470.
Jones, T. A., Zou, J. Y., Cowan, S. W. & Kjeldgaard, M. (1991). *Acta Cryst.* A**47**, 110–119.
Kojima, F., Naraba, H., Sasaki, Y., Beppu, M., Aoki, H. & Kawai, S. (2003). *Arthritis Rheum.* **48**, 2819–2828.
Laskowski, R., MacArthur, M., Moss, D. & Thornton, J. (1993). *J. Appl. Cryst.* **26**, 283–290.
Leistad, L., Feuerherm, A. J., Ostensen, M., Faxvaag, A. & Johansen, B. (2004). *Clin. Chem. Lab. Med.* **42**, 602–610.
Murshudov, G. N. & Dodson, E. J. (1997). *CCP4 Newsl.* **33**, 31–39.
Navaza, J. (1994). *Acta Cryst.* A**50**, 157–163.
Otwinowski, Z. & Minor, W. (1997). *Methods Enzymol.* **176**, 307–326.
Perbandt, M., Wilson, J. C., Eschenburg, S., Mancheva, I., Aleksiev, B., Genov, N., Willingmann, P., Weber, W., Singh, T. P. & Betzel, C. (1997). *FEBS Lett.* **412**, 573–577.

Ramachandran, G. N. & Sasisekaran, V. (1968). *Adv. Protein Chem.* **23**, 713–720.
Saiga, A., Morioka, Y., Ono, T., Nakano, K., Ishimoto, Y., Arita, H. & Hanasaki, K. (2001). *Biochim. Biophys. Acta*, **1530**, 67–76.
Schmitz, K. S. (1990). *An Introduction to Dynamic Light Scattering by Macromolecules.* Boston: Academic Press.
Schulze, T. (1996). Diploma Thesis, University of Hamburg, Hamburg, Germany.
Singh, N., Jabeen, T., Somvanshi, R. K., Sharma, S. & Singh, T. P. (2004). *Biochemistry*, **43**, 14577–14583.
Singh, R. K., Vikram, P., Makker, J., Jabeen, T., Sharma, S., Dey, S., Kaur, P., Srinivasan, A. & Singh, T. P. (2003). *Biochemistry*, **42**, 11701–11706.
Zurier, R. B. (1975). *Ann. Clin. Lab. Sci.* **5**, 276–281.